Identification and characterisation of rock mass discontinuity sets using 3D laser scanning

BART VAN KNAPEN[1] & SIEFKO SLOB[2]

[1] *Delft University of Technology. (e-mail: bartvanknapen@yahoo.com)*
[2] *ITC. (e-mail: slob@itc.nl)*

Abstract: In this research a methodology has been worked out to automate the identification and characterisation of rock mass discontinuity sets using 3D terrestrial laser scan data. With 3D laser scan surveys a dense point cloud is generated that represents the geometry of the scanned rock face in very high detail. Through 3D surface reconstruction techniques the original rock surface can be rebuilt in the form of a very large number of 3D facets. The normal vector data representing these 3D facets can be plotted as poles in a hemispherical projection. In order to avoid the subjective choice of discontinuity sets from such a kernel density distribution, this process has been automated using fuzzy k-means cluster analysis. An approach to the number of discontinuity sets in the normal vector data set is obtained using cluster validity indices. Any apparent outliers that are present in the clusters determined are rejected based on statistics, assuming a circular distribution about the mean orientation. All facets that still contribute to a (delimited) cluster are used to extract the individual 3D 'virtual' rock surfaces and corresponding point clouds within each discontinuity set. A straightforward algorithm has been developed for this. By fitting planes to these point cloud data using Principal Component Analysis, it is possible to determine the intersection distances of the discontinuities with a line of any orientation (discontinuity spacing analysis). With this method, it is shown that (near) planar rock surfaces of discontinuity sets captured by the laser scanner can be identified and extracted as point cloud or facet surface data. This is supported visually by colouring the 'virtual' 3D rock surface according to the delimited clustering results. The extracted 3D rock surface data can serve as a basis for many other discontinuity surface analyses, such as set spacing, block size distribution, and in future research possibly even roughness.

Résumé: Dans ce projet de recherche, une méthodologie a été élaborée pour automatiser l'identification et la caractérisation des familles de discontinuités en utilisant des données de scanner laser 3D. Lors de l'acquisition de données de scanner laser, on génère un nuage de points dense qui représente en détail la géométrie de la face rocheuse scannée. Par des techniques de reconstruction, la surface d'origine peut être reconstruite sous forme d'un très grand nombre de facettes. Les normales à ces facettes 3D peuvent être représentées comme les pôles d'une projection hémisphérique. Pour éviter toute subjectivité, le choix des familles de discontinuités à partir d'une telle distribution a été automatisé en utilisant l'analyse du groupement des données flou. Le nombre de discontinuités a été déterminé à partir d'indices de validité de groupement. Tout point aberrant présent dans les groupes a été rejeté en faisant l'hypothèse d'une distribution circulaire autour de l'orientation moyenne. Toutes les facettes qui contribuent encore à un groupe (délimité) ont été utilisées pour extraire les surfaces rocheuses virtuelles pour chaque famille de discontinuités et les nuages de points leur correspondant. Un algorithme a été développé pour cela. En ajustant des plans à travers ces nuages de points par l'analyse en composantes principales, il a été possible de déterminer la distance d'intersection entre les discontinuités et une ligne d'une orientation donnée (analyse d'espacement entre discontinuités). Par cette méthode, on a montré que les surfaces de familles de discontinuités presque planes peuvent être capturées à l'aide du scanner laser, identifiées et extraites sous forme de nuages de points ou de facettes. Un support visuel est apporté par le coloriage de la face rocheuse virtuelle selon le résultat du groupement délimité. Les données 3D extraites des surfaces rocheuses peuvent servir de base à bien d'autres analyses de surface de discontinuités telles que celles de l'espacement entre discontinuités, de la taille de blocs et dans le future, de la rugosité des discontinuités.

Keywords: 3D models, discontinuities, remote sensing, rock description, data analysis, data visualisation

INTRODUCTION

In this research a method has been worked to automate the identification and characterisation of rock mass discontinuity sets using 3D terrestrial (ground-based) laser scan data. Ground-based laser scanning is an emerging technology offering great potential for a rapid collection of dense, three-dimensional (3D) spatial data sets of any object, including rock surfaces. The proposed technique could give the site engineer or geologist, in real-time, evidence on the internal structure and insight into the mechanical behaviour of any discontinuous rock mass. Particularly in areas where access to rock outcrops is poor, application of this technique will be very promising.

© The Geological Society of London 2006

DISCONTINUITY MEASUREMENTS

Manual methods

It is generally accepted in the engineering geological community that discontinuities play a major role in projects that involve discontinuous rock masses. Particularly the characterisation of the discontinuities (orientation, number of sets, spacing, persistence, roughness) is very important in the design and construction phase for tunnels, foundations, excavations and slope stability analysis. Traditionally, a structured recording of discontinuity properties of a rock mass is achieved by conducting a scanline survey or cell mapping (Priest & Hudson, 1981; Priest, 1993). The measurement of discontinuity orientation and position at exposed rock faces is carried out using hand-held equipment such as a geological compass-clinometer device and measuring tape.

In most cases, the process of measuring requires physical contact with the exposed rock mass, mostly along the base of a slope. This has great influence on the quality and quantity of orientation measurements, and may also involve safety risks:

Quality and quantity of the measurements

- Only the base of the slope is considered, a large part of the exposure may be beyond normal reach and simply inaccessible, or only with scaffold or by rock climbing;
- There are large sources of error in gathering field discontinuity data, caused by sampling difficulties, choice of sampling method, human bias, instrument error, etc. Some examples:
  - Taking measurements by hand is a tedious and time-consuming process, often resulting in gross errors and blunders due to fatigue or diminished concentration;
  - Inaccuracies in the compass measurement may involve an error in the reading and the positioning of the instrument. Windsor & Robertson (1994) expect these errors to be around 5º for dip angle and around 10º for dip direction. Einstein & Baecher (1983) addressed the problem that the variance of dip direction measurements is much greater for horizontal planes than for steeper planes. Although quantity of the orientation measurements might be improved by the use of an electronic compass, there may still be an error in positioning the compass;
  - The part of the rock surface that is sampled is often different from the zone of interest, and may be affected by features such as blasting damage, degradation by weathering or a vegetation cover;
  - If a discontinuity surface is rough and wavy, measurements of its orientation will vary from one spot to another as the compass device can only measure a limited area of the exposed surface. This error might be reduced with the use of discs with increasing diameter as illustrated in Fecker & Rengers (1971), Hoek (1972) and ISRM (1981).

Safety risk:

- Often field measurements have to be carried out during potentially dangerous quarrying, tunnelling or mining operations or along busy highways or railway lines;
- Rock slopes are often dangerous because of rock fall.

3D terrestrial laser-scanning as an alternative measuring technique

Recent studies by for example Reid & Harrison, 2000; Feng et al 2001; Fasching et al., 2001; Kemeny & Post, 2003; Slob et al., 2004; Trinks et al. 2005; and Kemeny & Donovan, 2005, have already demonstrated that 3D laser scanning is a promising remote sensing technique to gather, from a safe distance, highly accurate discontinuity measurements. This paper demonstrates that it will also be possible to automate the processing of the data.

3D terrestrial laser scanning is a relatively new, but already revolutionary, surveying technique. The main advantage over for example photogrammetric remote sensing techniques is that a 3D data model is generated in real-time. Different laser scanning systems exist, but the technique used outdoors for geodetic surveying or for measuring large civil engineering structures is usually the 'time-of-flight' or 'laser range finding' technique.

During a laser-ranging survey, the laser periodically emits narrow pulses of near infrared light that are reflected by the rock face. These measurements are instantaneously translated into xyz-coordinates, relative to the scanner's position, using the two-way time-of-flight for each received pulse. This results in a real-time acquisition of a dense 3D point cloud of the rock surface (commonly over one million points), which contains information about the surface topography and therefore, the discontinuity surfaces of the rock mass. The xyz data can be added with the return signal amplitude for each pulse (intensity), or with colour (red, green, blue) information extracted from digital imagery.

DATA PROCESSING AND VISUALISATION

Surface reconstruction

The processing of the raw (x,y,z) data starts with a surface reconstruction to either a simplicial representation (Delaunay triangulation) or an implicit representation (Radial Basis Functions, RBF). Both methods generate meshed surfaces that consist of facets (e.g. triangles) and vertices that represent the rock surface morphology in high detail.

Since each (triangular) facet corresponds to (three) vertices of known (x,y,z) coordinates, the normal vector of all facets can be determined easily using basic geometric rules. Thus, this normal vector to each facet can be considered as an orientation measurement, assuming that this facet is indeed part of a discontinuity surface. Since we often have several thousands to millions of facets in our reconstructed, "virtual" rock surface, we can safely carry out (cluster) statistical analyses with this orientation data in order to find the trends.

Cluster analysis of the laser-derived orientation data

The directional data (in fact, the normals from the facets) is used as input for fuzzy k-means clustering based on eigenanalysis, which allows for a quick identification of different clusters or discontinuity sets. By using validity indices (e.g. Xie-Beni, Fukuyama-Sugeno and fuzzy hypervolume) to determine the number of clusters, the process of identification is kept as objective as possible.

Fuzzy k-means clustering

The fuzzy k-means clustering algorithm (also known as fuzzy c-means or fcm) is a supervised classification, for which the number of final clusters has to be determined in advance, based on the validity indices. The fuzzy k-means clustering algorithm is based on a so-called "soft" clustering scheme and partitions the data set according to the degrees of membership assigned to a set. The degree of membership ranges from zero to one and the greater the certainty that a data point belongs to a set, the closer its membership value is to one. This concept was put forward in the sixties (Zadeh, 1965) and it took over 25 years to be applied to the analysis of discontinuity data (Harrison, 1992). Fuzzy set theory is a means to account for uncertainty in data in a realistic and natural manner (Bezdek, 1981) and is successfully applied in fields of pattern recognition, image processing and neural networks (Zhou & Maerz, 2002).

It should be noted that any clustering algorithm assumes a certain structure in a data set, which does not necessarily reflect the actual cluster structure. The incorporated distance-metric in fuzzy k-means clustering forces the algorithm to seek primarily for rotationally symmetric clusters. However, non-circular (e.g. elliptical) clusters that are well separated and equally distributed with respect to each other can also be isolated.

Cluster validity

In order to assess the results of the data partitioning with fuzzy k-means clustering, fuzzy validity indices have been developed (Xie & Beni, 1991; Gath & Geva, 1989). Another way to use these indices is to get an indication about the number of clusters prior to the partitioning of the data. For orientation data, adjusted validity index functions need to be applied as put forward by Hammah & Curran (2000).

Directly related to the definition of a cluster is the basic assumption that clusters are by definition present in the data. The correctness of the data set partitioning and the use of validity indices therefore depend on the existence, as well as the distribution of the trends in the data. For example, it is possible that different validity indices give different indications to the number of clusters, which mainly depends on the data distribution density and separation of the clusters, if present. In addition, it should be noted that only the orientation data is used for clustering and subsequently tested for validity, although this should actually be extended to incorporate other discontinuity parameters such as spacing or roughness.

Cluster statistics

After the fuzzy k-means clustering, the identified sets can be statistically analysed. This is to acquire statistical information on the distribution density of the recognised clusters. The distribution of orientations is assumed to be circular and rotationally symmetric, therefore following a Fisher Distribution. The clusters are delineated by the assigned membership values during the execution of the fuzzy k-means clustering algorithm. A cluster number is given to each discontinuity set corresponding to the highest membership contribution (between 0 and 1).

Cluster visualisation

The resulting clusters can either be visualised in a stereonet representation by the facet's poles or by giving each 3D facet a colour in 3D space representing the cluster to which it belongs. The latter option gives a good impression of the validity of the results, since the reconstructed rock surface is coloured according to the discontinuity set it belongs to. For each discontinuity set, parameters and statistics are determined, such as: mean orientation, number of facets, total rock surface area, concentration parameter, spherical variance, eigenvalues, and mean resultant vector length. As in all natural data sets, occurrence of noisy data is expected (due to vegetation, weathered surfaces or loose slope material, for example). Each cluster will therefore to some extent contain cluster outliers, which are facets that have an orientation that falls outside a specified region from the cluster mean orientation (centre). These data will affect the cluster statistics, such as the mean orientation. However, these cluster outliers can be rejected, and their effect minimised, based on their distance to the cluster centre, or changes in statistic parameters mentioned (e.g. an increase of concentration parameter).

Delimiting clusters

After the statistical clustering, the results may not correspond to how the data is visually and intuitively perceived by the user. It is possible that a cluster represents both vertical and horizontal surfaces or that the cluster centre has a visually identifiable shift from its apparent location. In some cases, the presence of cluster outliers or noise in the data can be the reason for this. For an improvement of the correctness, reliability, and interpretability of the data it is therefore highly recommended to remove these obvious outliers.

The rejection criteria proposed here to delimit clusters, are all based on the unit distance of the initially clustered data to their respective cluster centres. In an iterative scheme small distance steps are subtracted from the maximum distance, or the maximum extension found for the cluster. Any data point (unit normal vector) from which the distance is found to be below the iterative distance, will be treated as a cluster outlier or 'noise' and excluded from further analysis. Subsequent to each cluster delimitation or iteration, new cluster centres are calculated.

If the newly defined clusters are visually acceptable, cluster statistics can again be used to validate and verify whether the clustering has indeed improved. It should be noted however, that some initial values will differ from the newly determined values, such as the eigenvalues and cluster mean normals. These initial values were determined with weights based on the degree of membership, which depends on all other clusters present. Since the clusters are treated separately from each other during the outlier rejection, all members will in fact have a membership value of 1.

De-clustering to single discontinuity surfaces

For the automated detection of individual discontinuity surfaces, the topologic relationship between the facets in 3D space is used. Neighbouring facets have at least one vertex in common, which allows for a reconstruction of the discontinuity surface. Here the (delimited) clustering results are used as outer boundaries of allowable orientation deviations, instead of taking the entire data set with a threshold for maximum orientation deviation. This saves a lot of computing time. The obtained surfaces are further processed by removal of very small surfaces, which mostly consists of only a few facets. The resulting data set of vertices for each surface serves as input for Principal Component Analysis (PCA), in which the best-fit planes are computed, as well as some other statistics, such as the eigenvectors, multiple correlation coefficient, sum of residuals, and discontinuity surface dimensions.

The resulting planes of best fit that represent the relatively larger discontinuity surfaces of each discontinuity set within the selected data set, are used to obtain discontinuity set characteristics, in particular normal set spacing and total spacing distributions. In this automated approach built-in thresholds and assumptions on surface continuity are set to reduce potential errors in the final results.

Data and processing errors

During the processing and analysis of the raw laser scan data, several errors need to be accounted for. Since different processes and assumptions are involved, it is difficult to quantify the accuracy of the defined discontinuity characteristics. During laser survey data acquisition, the laser scan system will always be prone to small errors, which depend upon the laser system characteristic parameters, such as the angular accuracy, beam divergence and range accuracy. Moreover, the acquired data will be susceptible to noise as a result of unwanted features, such as vegetation, passing vehicles or birds. Other errors are involved in the surface reconstruction technique applied (smoothening, edges, low density regions, etc.), the data selection (crop) made for analysis ('shadow zone', under- and overrepresented sets), the number of scan positions involved in analysis (to improve accuracy and validate consistency of results), and the clustering technique applied (assuming a circular Fisher distribution around the mean).

VALIDATION USING FIELD DATA

In search for a validation of the proposed method, manual and laser scan surveys have been carried out at localities in Spain, from which, for this study, one site was selected as an example. For this case, one sub-data set (crop) was selected from a larger laser scan data set of an entire rock slope. The data set has been georeferenced (levelled and aligned with respect to the magnetic North). Only in this way can the measurements be properly compared with the magnetic compass measurements. The automated identification of discontinuity sets was found to be visually correct and even revealed sets that remained unrecognised during the manual scanline survey (sets parallel to the scanline). On the other hand, some discontinuity sets may still be partitioned further, for example based on surface roughness characteristics. Analysis of more crop selections, preferably from data sets acquired at different scan positions, should be done to validate this.

The case study is from a rock exposure along the road TP7403 (at marker km06) between Torroja del Priorat and Porrera, Priorat district, Catalan Province, Spain (Figure 1, Left). The rock exposure consists of a slightly weathered, greyish, medium-grained, blocky, moderately strong META-SANDSTONE[1], and dates from the Carboniferous. The dimension of the exposed rock surface is about 12 x 4 x 3 m (width, height, depth).

Manual survey results

From a horizontal scanline of 5.9 m and two vertical scanlines of 1.9 m and 1.5 m, the measured orientations have been weighted and plotted in an equal area hemispherical projection net. Based on the contoured kernel density plot of the weighted data (Figure 2, left), five major discontinuity sets were identified (Figure 2, right). Table 1 lists the statistics for each discontinuity set.

From the 5 major discontinuity sets identified, the bedding planes B1, and joint set J2 are represented by many measurements as observed from the kernel density plot (Figure 2, left) and Table 1. It is expected that these discontinuity sets will be identified from the laser scan data, regardless of the laser scan data set selected. Discontinuity sets J4 and J5 can not only be separated based on their dip angles, but also on their difference in large-scale roughness values which range from straight (J5) to curved[2] (J4) (Figure 3). Since this roughness has not been

[1] Medium-grained metamorphic rock formed from sandstone
[2] SSPC system (Hack, 1998)

incorporated in the clustering process, these discontinuity sets are probably recognised as one set. Discontinuity set J3 consists of only 3 measurements (9 when weighted), but visually forms a separate set.

Figure 1. Photograph of the studied rock exposures. It is a meta-sandstone from the Carboniferous period. Part of this slope (outlined with the square and shown in more detail on the right) is used as a case study in this section. The two boards in the picture were used to georeference the laser scan data set. Location: road TP7403 (km06) between Torroja del Priorat and Porrera, Priorat district, Catalan Province, Spain.

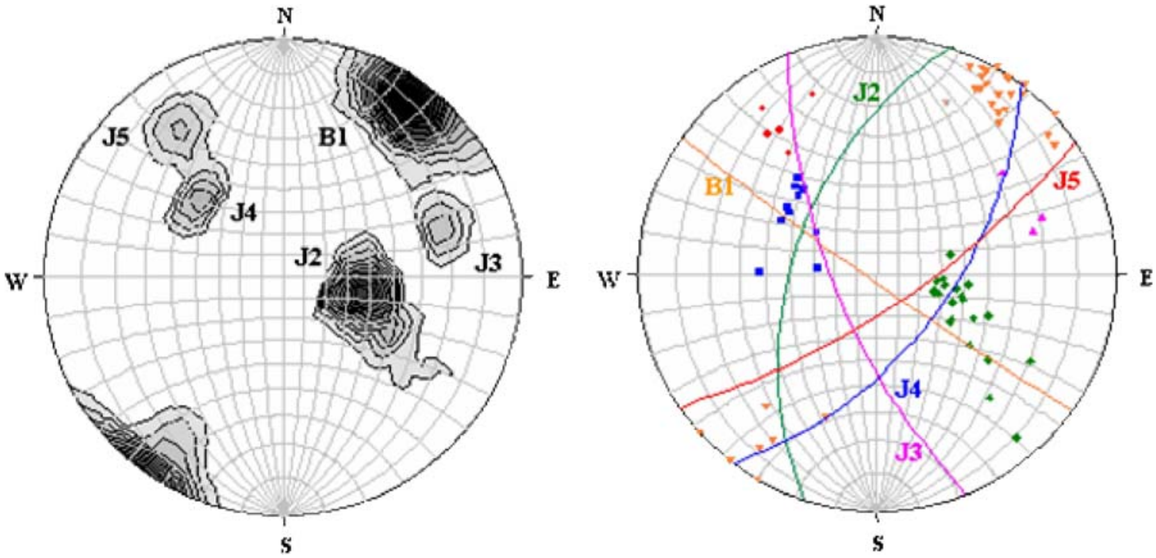

Figure 2. Left: Kernel density plot of weighted orientation data (poles) of 3 scanline surveys. Right: Identified discontinuity sets given by a coloured symbol, while identifiers denote the mean great circle of a set. Table 1 lists statistic characteristics for each set. Both plots are obtained with the program Stereo Nett by Duyster (2000).

Laser scan survey results

The laser scan survey has been performed with an Ilris-3D laser scanning system (Ilris, 2004) from one scan position. One crop that consists of over 75,000 points has been selected from the laser scan data set for further analysis (representing the area show in Figure 1, right). This point cloud data has been reconstructed using Radial Basis Functions (RBF) in the program FastRBF (Farfield technology, 2004) with a smoothing of 1 cm. In order to compare the obtained orientation distributions with the manual data, the xyz-data have been georeferenced (to magnetic North) using the measured orientations of the two boards present in the laser scan window. The smallest error as a result of rotation found for this data set is 2 degrees in dip direction and 0.5 degrees in dip angle.

Table 1. Discontinuity set (statistic) characteristics

	B1	J2	J3	J4	J5
Dip direction [°]	215	288	248	127	146
Dip angle [°]	86	41	69	47	73
Dip direction range [°]	200-234	255-318	231-255	091-140	142-160
Dip angle range [°]	72-90	28-84	68-72	28-55	64-80
Spherical variance [°]	0.01527959	0.03438402	0.01068670	0.02296123	0.00616270
θ_{95} [°]	2.3125	3.3239	5.4702	6.1240	4.4868
P(<θ), θ= 5 [% of N]	> 0.95	0.1016	0.2419	0.1324	0.3707
Mean res. vector length	0.9689	0.9301	0.9756	0.9503	0.9856
Conc. parameter (κ)	63.19	28.16	72.78	37.33	121.7
# weighted N	58	63	9	14	8

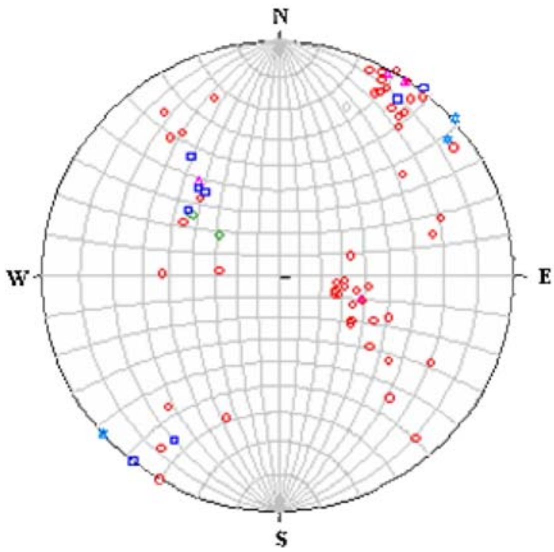

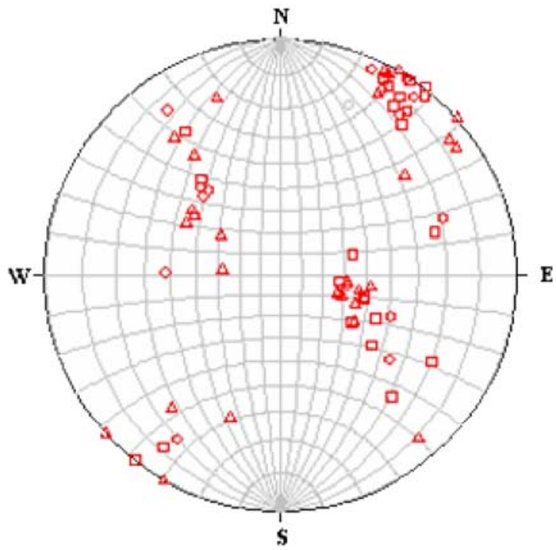

Figure 3. Left: Attribute plot of large-scale roughness (SSPC) obtained from the scanline surveys, where distinction is made between straight (red circle), slightly curved (blue rectangle), curved (purple triangle), slightly wavy (green spade), and wavy (light blue star). Note that all surface traces < 1.0m are straight in a SSPC. Right: Small-scale roughness recordings. Rough, smooth and polished are respectively red, blue and purple. Stepped, undulating and planar are represented by a rectangle, triangle, circle symbol respectively. All small-scale roughness values recorded are rough in this case. Both plots are obtained with the program Stereo Nett by Duyster (2000).

Determination of clusters

For an optimal partition of the normal vector data set, the validity indices are used as an estimate to the number of clusters (Figure 4). Although the Xie-Beni index and Fukuyama-Sugeno index indicate that the best partitioning is achieved with 4 clusters, the other indices point towards their second-best indication of 5 clusters. Accordingly, this has been used as input to the fuzzy k-means clustering algorithm, from which the results have been plotted as poles in a lower hemispherical equal-area projection (Figure 5). The manual orientation data is plotted in the same projection with white diamonds.

Because this laser scan data set is relatively small it was also possible to use the software DIPS (Rocscience Inc., 2004) to create a kernel density plot (Figure 6). Although it took the program about 20 minutes to process the large number of data points, it finally gives a good comparison of mean orientations with the clustering results (Table 2). Comparison of Figure 5 and Figure 6 show that the kernel density plot visually divides the orientation data in the same clusters as done in an automated fashion by the clustering algorithm.

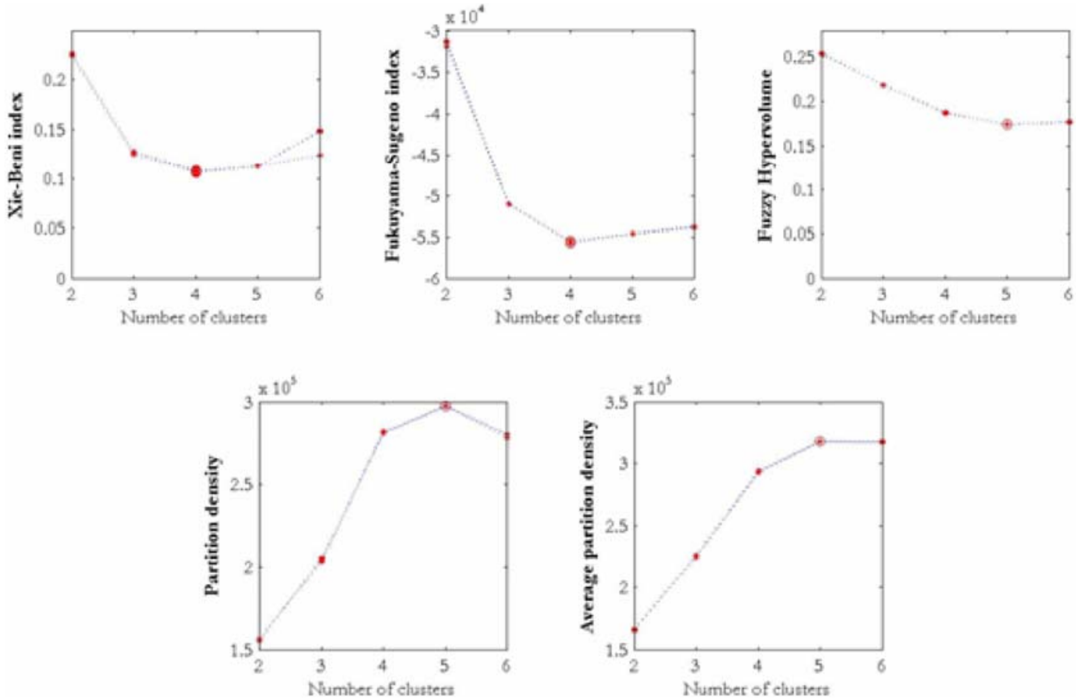

Figure 4. Validity indices for the data set in this case study. The lines in each graph correspond to different partitions, which have been performed 3 times in an iterative scheme. The Xie-Beni index and Fukuyama-Sugeno index both indicate that 4 clusters give the best partition of the normal vector data, while the other indices indicate 5 clusters as the best partition. Since the second-best indication of the Xie-Beni index and Fukuyama-Sugeno index is 5 clusters, this is chosen.

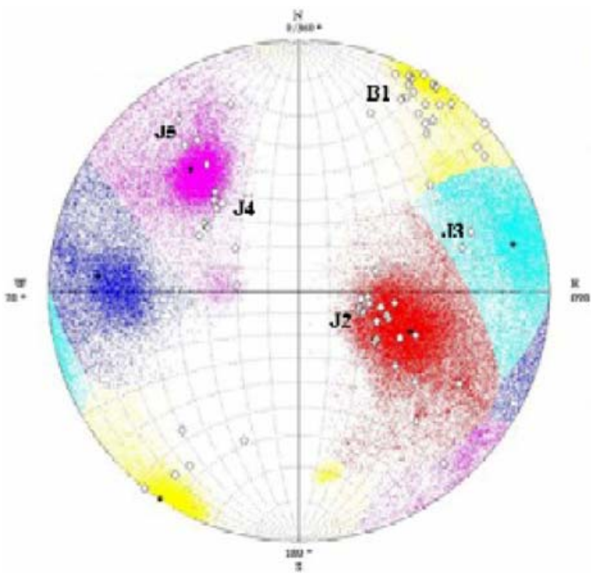

Figure 5. Equal area hemispherical projection of all facet poles grouped using fuzzy k-means clustering. Based on the validity indices, 5 clusters were used as input. The scanline orientation data is also represented by poles (white diamonds). Obviously, the yellow, red, and purple discontinuity sets were identified. Note that the blue (and to some extent cyan) cluster has not been recognised during the scanline survey (parallel to scanline). The rock surface area is around 2.6 m^2. The laser scan data has been rotated around 093/02.

Colouring the rock surface

Based on the clustering results, the rock surface has been coloured by giving each facet the colour of its respective cluster (Figure 7, left). The clusters have been delimited to remove outliers and to reduce the cluster centre (mean orientation) offset (Figure 8 and Figure 7, right). The cluster statistics for the delimited clusters are given in Table 2 by the underlined values. Although this removes a lot of random orientations, there is also a part of the rock surface that appears to be part of another discontinuity set having an orientation of about 350/80 (yellow).

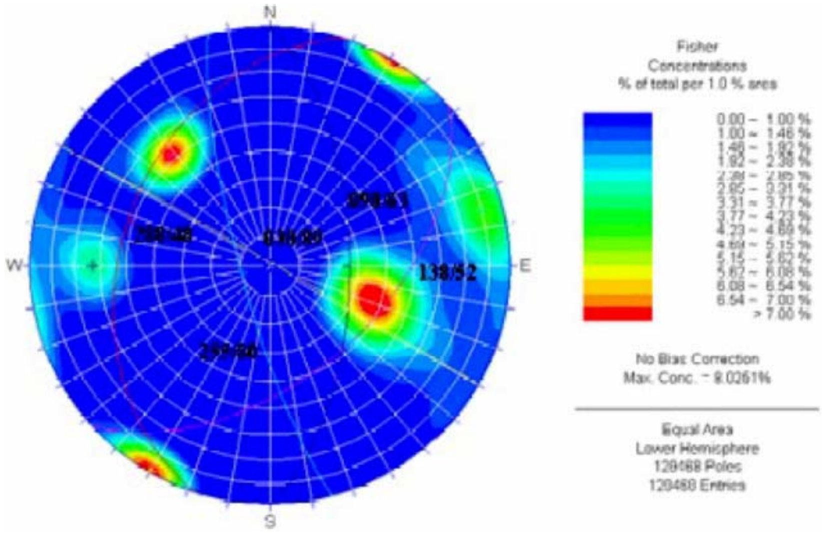

Figure 6. Kernel density plot of all 129,468 facet poles with the program DIPS (Rocscience Inc., 2004). The displayed orientations based on these distributions were added manually later. The mean orientations from this plot and those obtained from clustering are listed in table 2.

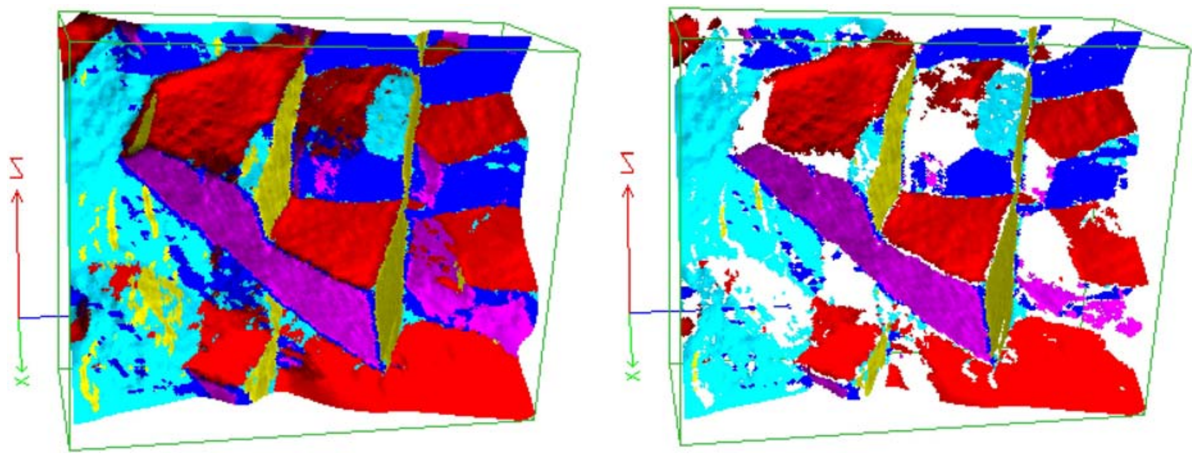

Figure 7. Left: Coloured reconstructed rock. Right: Coloured reconstructed rock surface without rejected facets. Note the yellow surface patch on the upper left block, which is probably part of another discontinuity set but rejected here. Also note the blue band surrounding the large purple surface, which is the result of smoothing the edge.

Extraction of individual surfaces

The remaining facets after delimitation (Figure 7, right) are used to extract the different surfaces by finding all neighbours in a repetitive scheme of iterations. In Table 2, the number of individual (not interconnected) surfaces is listed for each cluster separately. The number of surfaces remaining after rejecting the relatively smaller surfaces is underlined in the table. In particular, discontinuity set J3 (cyan colour) seems to consist of many single facets or small surface patches.

Discussion of results

Again, the results have shown that the applied methodology is able to extract the major discontinuity sets based on their orientation. Although slight differences in mean orientation occur with the discontinuity sets recognised in the scanline survey, the colouring of the rock surface visually shows that the larger surfaces are identified correctly. Discontinuity sets B1 and J2 were identified easily from the laser scan data. Another major discontinuity set (J6, blue) was identified, while it remained unnoticed during the scanline survey. A simple explanation for this is that the discontinuity surfaces of this set are oriented parallel to both the horizontal and vertical scanlines performed (i.e. mean set normal is near perpendicular to all scanline orientations) and are therefore missed.

Table 2. Discontinuity set statistics resulting from fuzzy k-means clustering. The underlined values represent statistics after delimitation of the cluster. Note that the order of manually detected discontinuity sets of table 1 is maintained here, that 2 discontinuity sets (J4 & J5) identified from the scanline survey data are merged into one, and that one undiscovered discontinuity set has been identified in this particular laser data set (J6).

	B1	J2	J3	J4 J5	J6 (new)
Cluster number	3 (yellow)	2 (red)	5 (cyan)	4 (purple)	1 (blue)
Initial orientation [°]	032/89	289/38	257/80	139/52	092/65
Orientation after delimitation [°]	034/90	290/39	258/77	138/55	094/69
DIPS mean orientation [°]	030/89	288/48	255/80	138/52	090/63
Scanline orientation [°]	215/86	288/41	248/69	127/47 146/73	--
Spherical variance [°]	0.10209 0.007645	0.044972 0.023458	0.035661 0.016318	0.055462 0.010957	0.048178 0.021087
Mean res. vector length	0.89791 0.99235	0.95503 0.97654	0.96434 0.98368	0.94454 0.98904	0.95182 0.97891
Conc. parameter (κ)	9.7947 130.782	22.2349 42.6277	28.0395 61.2746	18.0288 91.2574	20.7541 47.4156
Number of data points (facets)(N)	20067 14652	41601 33747	23839 16106	25371 17422	18590 12771
Approx. surface area [m^2]	0.40137 0.29071	0.86515 0.69792	0.44932 0.29556	0.50755 0.34762	0.37718 0.25501
Number of individual surfaces	23 4	72 10	172 5	42 5	147 20

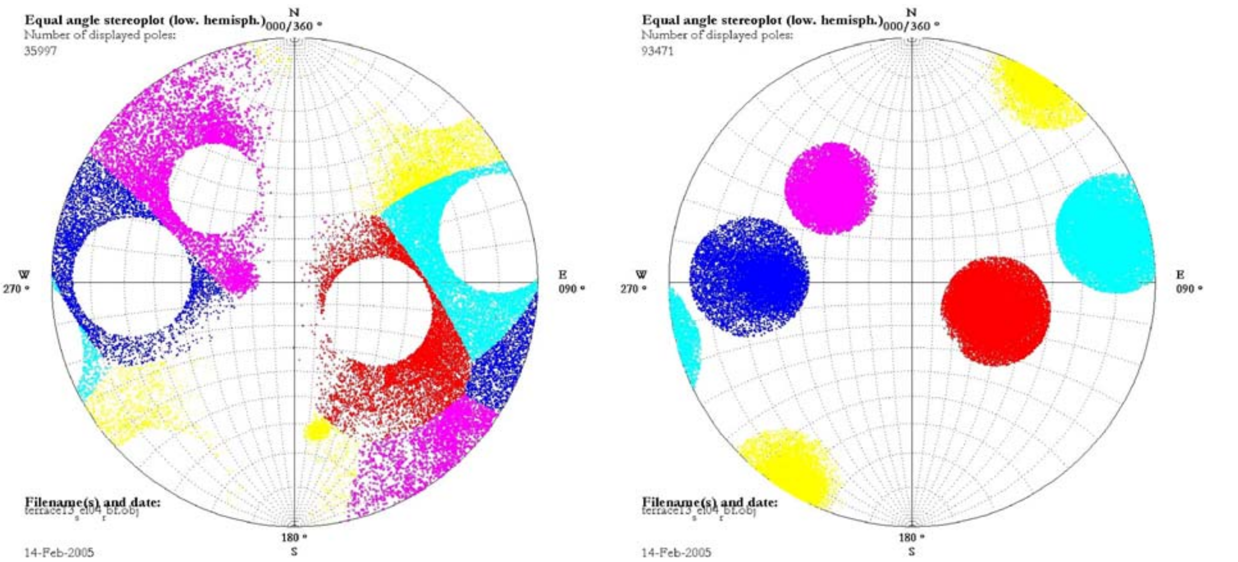

Figure 8. Lower hemispherical equal angle projection of rejected poles or cluster outliers (left) and the remaining high-density circular distributions of clustered poles (right). The number of rejected poles is 35,997 (28%), whereas 93,471 poles are maintained. The arrows indicates rejected poles that are most likely part of a rock surface that represents an under-represented discontinuity set.

As was expected, sets J4 and J5 were not recognised as separate clusters, simply because the difference in mean orientation, as well as the data density differences are too small to allow for partition into separated clusters. However, another crop selection should be analysed to validate their presence from the laser scan data. Discontinuity set J3, that consists of only three observations is most likely also underrepresented in the laser scan crop selection. Again, more crop selections from other parts of the rock exposure, preferably from different laser scan positions, will be needed to enable the identification of this discontinuity set.

In the laser scan data some smaller rock surfaces or patches were observed as small clusters in the orientation data. These (single) surfaces were underrepresented in this crop selection and consequently rejected during cluster delimitation. It is however thought that these sets can be identified and extracted from other crop selections.

CONCLUSIONS

In this research a method has been worked out to automate the identification and characterisation of rock mass discontinuity sets using 3D terrestrial laser scan data. It is demonstrated that 3D laser scanning data can be used as a tool to:

- Rapidly acquire a model of rock slopes at high detail and with high accuracy in 3D with 3D Delaunay triangulation and Radial Basis Functions (RBF) surface reconstruction techniques;
- Determine orientations of discontinuity sets of an exposed discontinuous rock mass from this modelled rock surface without physical access to the slope;
- Automate discontinuity set identification using fuzzy k-means clustering;
- Visualise the results in the 3D 'virtual' rock surface model by unique colours obtained for clustering;
- Automate the identification, extraction and analysis of individual discontinuity set surfaces;

Acknowledgements: This research is funded by ITC's internal research budget within the framework of the HiRES3D research program. The authors acknowledge John Kemeny from Split Engineering LCC for supplying the Ilris laser scanner for use during the fieldwork in Spain. Many thanks to John as well for using the beta version of the Fx software.

Corresponding author: Mr Siefko Slob, ITC, Hengelosestraat 99, Enschede, Overijssel, 7500 AA, Netherlands. Tel: +31 53 4874444. Email: slob@itc.nl.

REFERENCES

BEZDEK, J.C., 1981. Pattern recognition with fuzzy objective function algorithms. Plenum, New York.

DUYSTER, J., 2000. Stereo Nett Version 2.46, Ruhr University Bochum. Download at: http://homepage.ruhr-uni-bochum.de/Johannes.P.Duyster/stereo/stereo1.htm. Last assessed December 2004.

EINSTEIN, H.H. & BAECHER, G.B., 1983. Probabilistic and statistical methods in engineering geology. Specific methods and examples. Part I: Exploration. *Rock mechanics and rock engineering,* Vol. **16** (1983), pp. 73-79.

FARFIELD TECHNOLOGY, 2004. About the Points2Polys software: http://www.farfieldtechnology.com/products. Last assessed December 2004.

FASCHING, A., GAICH, A. AND SCHUBERT, W. 2001. Data acquisition in Engineering Geology. An improvement of Acquisition Methods for Geotechnical Rock Mass Parameters. *Felsbau* 19 (2001) Nr. **5**., pp. 93-101.

FECKER, E. & RENGERS, N., 1971. Measurement of large scale roughness of rock planes by means of profilograph and geological compass. *Rock fracture, Proc. of Int. Symp. Rock Mech.,* Nancy, Paper I-18.

FENG, Q., SJÖGREN, P., STEPHANSSON, O. AND JING, L. 2001. Measuring fracture orientation at exposed rock faces by using a non-reflector total station. *Engineering Geology* **59**, pp. 133-146.

GATH, I. & GEVA, A.B. 1989. Unsupervised optimal fuzzy clustering. *IEEE Trans. Pattern Anal. Machine Intell.* **11**(7), pp. 773-781.

HACK, H.R.G.K. 1998. Slope Stability Probability Calculation SSPC. ITC Publication Number 43. 2nd Version.

HAMMAH, R.E. & CURRAN, J.H., 2000. Validity Measures for the Fuzzy Cluster Analysis of Orientations. *IEEE Trans. on pattern analysis and machine intelligence*, Vol. **22** (12), pp. 1467-1472.

HARRISON, J.P., 1992. Fuzzy objective functions applied to the analysis of discontinuity orientation data. *In: Eurock'92*, pp. 25-30.

HOEK, E. 1972. Rock slope engineering, Rock slope stability in open cast mining, *Part 1 – Collection and interpretation of data required for slope analysis*, Imperial College, Rock Mechanics Progress Report, No. **8**, July, 1972, pp. 131.

ISRM 1981. Rock characterization, testing and monitoring. *ISRM Suggested Methods. Brown*, E.T. (ed.). Pergamon Press. 211 pp.

ILRIS 3D HOMEPAGE. 2004. Optech Incorporated. http://www.optech.on.ca/prodilris.htm. Last assessed December 2004.

KEMENY, J. & DONOVAN, J. 2005. Rock mass discontinuity characterisation using LIDAR and automated point cloud processing. *Ground Engineering*, November 2005, 26-29.

KEMENY, J. & POST, R. 2003. Estimating three-dimensional rock discontinuity orientation from digital images of fracture traces. *Computers and Geosciences* Vol. **29**, pp. 65-77.

PRIEST, S.D. & HUDSON, J.A. 1981. Estimation of discontinuity spacing and trace length using scanline surveys. *Int. J. Rock Mech. Min. Sci. & Geomech. Abstr*. Vol **18**, pp. 183-197.

PRIEST, S.D. 1993. Discontinuity Analysis for Rock Engineering. Chapman & Hall, London, 473 pp.

REID, T.R. & HARRISON, J.P., 2000. A semi-automated methodology for discontinuity trace detection in digital images of rock mass exposures. . *Int. J. Rock Mech. Min. Sci* Vol. **37** (2000), pp. 1073-1089.

ROCSCIENCE INC., 2004. DIPS Version 5.0 (demo available free from charge) at: http://www.rocscience.com /products/Dips.asp. Last assessed December 2004.

SLOB, S., HACK, R., VAN KNAPEN, B., TURNER, A.K. & KEMENY, J. 2004. A method for automated discontinuity analysis of rock slopes with 3D laser scanning. *TRB annual meeting*, Washington, 2004.

TRINKS, I., CLEGG, P., MCCAFFREY, K., JONES, R., HOBBS, R., HOLDSWORTH, B., HOLLIMAN, N., IMBER, J., WAGGOTT, S., WILSON, R. 2005. Mapping and analyzing virtual outcrops. Visual Geosciences, DOI 10.1007/s10069-005-0026-9.

WINDSOR, C.R. AND ROBERTSON, W.V., 1994. Rock Reinforcement Practice, *Volume 1, Rock Mass Formulation.*

XIE, X.L. & BENI, G.A. 1991. A validity measure for fuzzy clustering. *IEEE Trans. Pattern Anal. Machine Intell.,* **13**(8), pp. 841-847.

ZADEH, L.A., 1965. Fuzzy sets. *Information Control* Vol**. 8** (3), pp. 338–353.

ZHOU, W. & MAERZ, N.H. 2002. Implementation of multivariate clustering methods for characterizing discontinuities data from scanlines and oriented boreholes. *Computers and Geosciences*, Vol. **28**, pp. 827-839.